University of Nevada, Reno

Developing Zeeman Broadening Diagnostics for Magnetized Plasmas

A thesis submitted in partial fulfillment
of the requirements for the degree of

Bachelor of Science in Physics and the Honors Program

by

Showera Haque

Radu Presura, Ph.D, Thesis Advisor

May, 2013

UNIVERSITY
OF NEVADA
RENO

THE HONORS PROGRAM

We recommend that the thesis
prepared under our supervision by

SHOWERA HAQUE

entitled

Developing Zeeman Broadening Diagnostics for Magnetized Plasmas

be accepted in partial fulfillment of the
requirements for the degree of

BACHELOR OF SCIENCE, PHYSICS

_____

Radu Presura, Ph.D., Thesis Advisor

_____

David Bennum, Ph.D., Thesis Reader

_____

Tamara Valentine, Ph.D., Director, Honors Program

May 2013

Abstract

One of the most important parameters in laboratory plasmas is the magnetic field (strength and orientation). For these studies to be relevant to astrophysics, proper characterization of the forces acting upon laboratory-produced plasmas is necessary in order to scale the results to be able to understand larger systems. However, the time and space scales characteristic for laser plasmas do not allow particularly useful magnetic field measurements. Current techniques are either insufficient or unsatisfactory; as either the field strength cannot be resolved or only spatially average results are given. A new technique for magnetic field determination via Zeeman broadening is being explored, which is valid in cases even when field orientation is not uniform, which is often the most applicable case.

Table of Contents

List of Figures

I. Introduction

1.1 Motivation

Any study of astrophysical or high-energy density physical phenomena must involve a study of plasma. Plasmas exist at temperatures high enough to ionize its constituent atoms. Plasma is an assembly of moving charged particles (ions and electrons) that interact with each other via electrostatic and magnetic forces. [1] Consequently, the study of magnetic fields is important in understanding plasma dynamics. Plasmas are affected by the internal magnetic fields self-generated by its moving charges or by plasma instabilities and non-uniformities, and also by the presence of external, time-varying magnetic fields. The mechanics instigated by the unique properties of plasmas may provide answers to many open questions in the sciences.

The interaction of the solar wind with the Earth's magnetic field is an example of one such plasma phenomenon of importance due to the impact it has on us. The magnetic field generated by the active core of the Earth protects all terrestrial objects—living and inanimate—from harmful solar radiation. Solar wind, or energetic plasma from the sun, is ejected towards us at high speeds but is usually deflected into outer space by our magnetic field. However, during periods of high solar activity, particularly energetic streams of particles are able to penetrate across the magnetic barrier and make their way towards Earth. Evidence of solar plasma entering our atmosphere is given by the aurora borealis at the poles, but a more detrimental consequence is the disturbance of satellites and electric grids. Because of our heavy dependence on satellites and electric power for communication, navigation, and defense, it is extremely advantageous to be

able to make these systems less susceptible to damage. Understanding the processes responsible can help us do so.

Exotic astrophysical objects, such as supernovae and neutron stars, can be categorized by the fields they create. Neutron stars are extremely dense stars with some of the largest magnetic fields detected in the known universe. [2] Studying matter under these extreme conditions is crucial to a full understanding of how the most elementary particles that make up the world around us behave.

A final example to demonstrate the importance of studying magnetic fields in plasma sciences is the energy crisis. Fusion is one solution to curb our dependence on limited fossil fuels and to limit pollution of the environment. Fusion reactions occur at the core of every active star and provide enormous amounts of energy at the cost of hydrogen as fuel. However, these reactions are only sustainable at extreme temperature and densities and it is for this reason that they are not easily reproducible on Earth. To obtain the necessary conditions, extensive plasma research must be done in order to control and benefit from the process.

1.2 Realization of Plasma Studies

Given both our physical separation to these objects and lack of accessibility to the magnetohydrodynamic regimes which engender their environments, it would seem that the study and ultimately the mastery of plasma systems is well out of our reach. Fortunately however, through the use of pulsed power machines and lasers, we can recreate these conditions in the laboratory. Specifically, at the University of Nevada-Reno's Nevada Terawatt Facility, we have access to a 1 MA pulsed power generator to produce magnetic fields tens of millions of times stronger than that at the surface of the

Earth and a 10 J laser to produce plasmas with density and temperature similar to those of stellar interiors. Through appropriate scaling of plasma parameters, laboratory-produced plasmas can be accurately modeled to many types of their otherworldly counterparts.

Many parameters control the evolution of a plasma, including density, temperature, composition and magnetic field. The strength and orientation of the latter are one of the most elusive to physicists. Laboratory plasmas are very short lived, usually on the order of tens to hundreds of nanoseconds, and are therefore difficult to diagnose. There are a few different methods employed for magnetic field measurement, including Faraday rotation, B-dot probes, and Zeeman spectroscopy. Several experiments are conducted at NTF which explore the dynamics of various astrophysical phenomena, but no reliable magnetic field measurements are available. Currently data is analyzed using theoretical support for the magnetic fields expected, but without experimental confirmation we have an incomplete study.

Faraday rotation yields magnetic field measurements by taking advantage of the way polarized light interacts with plasmas permeated by external magnetic fields. It works by sending a linearly polarized probe laser beam through plasma and measuring the degree by which the plane of polarization of the laser light is rotated as the beam traverses the plasma. This measured angle of rotation will be proportional to the magnitude of the magnetic field present. One shortcoming of this method is that the information encoded about the magnetic field is in fact averaged over the length of the path the beam travelled through the plasma. Also, the data provides information only about fields aligned with the laser beam path. In the case of laser-produced plasmas,

because of the short time scales and high energies involved, very rarely are we able to study a specimen with a uniform magnetic field.

Another method for determining magnetic fields in plasma is spectroscopy. Spectroscopy is one type of study of emitted light from a source. Using prisms or diffraction gratings, the light can be dispersed in space as a function of wavelength. By examining what energy levels are excited at a given instant in time, we can discern information about what ions are actually present, temperature, and electromagnetic fields. When a plasma contains a magnetic field, some energy levels of the ions in that plasma are split, and transitions that normally would not be distinguishable are observed. This is known as the Zeeman Effect, and the magnitude of energy level displacements is proportional to the field present. Much like the Faraday rotation technique described above, the Zeeman splitting can be used to measure average values of uniform magnetic fields. In the presence of other spectrum-altering effects, often characteristic of the plasmas of interest, the Zeeman Effect can be drowned out, giving inconclusive measurements.

In light of the inadequacies of known methods for measuring magnetic fields in the laboratory, new avenues are being explored. One solution is called Zeeman broadening and was recently proposed by Israeli research team led by S. Tessarin. [3] This new spectroscopic technique not only allows measuring magnetic fields with spatially alternating orientation, but can take measurements of the magnetic field even when its effects on the spectrum are small when compared with those of other plasma parameters.

The goal of the present work is to develop a spectroscopic diagnostic utilizing Zeeman broadening to measure magnetic fields in regions with small-scale fluctuations of the field magnitude and orientation.

II. Theory

Before presenting in more detail the Zeeman broadening technique, first the basic Zeeman Effect must be understood and the reasons why it is not sufficient for our methods. The Zeeman Effect is observed through atomic radiation, so we begin by first explaining how atoms radiate in the absence of external perturbations.[1]

2.1 The Radiating Atom

Atomic systems are described by wavefunctions that are solutions to the Schrödinger equation. The wavefunction is a function of complex variables mapping the position of the electron in space and time. One of the postulates of quantum mechanics is that all observed states are eigenvalues of a certain operator acting on the wavefunction, ψ. The Hamiltonian operator, H, which expresses the total (potential and kinetic) energy of a system, acting upon a wavefunction returns the energy of that particular wavefunction. This equation is called the time-independent Schrödinger equation.

$$H\psi = E\psi$$

where E is the energy of ψ when placed in a system with total energy H. This equation only has a discrete set of wavefunctions that form the solution set, $\{\psi_n \mid n \in \mathbb{N}\}$. Each ψ_n then has its associated energy, E_n. The solutions to the time-independent

[1] A more rigorous treatment of perturbations to atomic systems by magnetic fields can be found in any textbook on quantum mechanics. The main sources of reference drawn from in the following section are Introduction to Quantum Mechanics by D.J. Griffiths and Introduction to Modern Optics by G.R. Fowles.

Schrödinger equation form a spectrum of allowable wavefunctions for an atomic system, which in turn forms a spectrum of allowable energies for an atomic system. This is specific to quantum mechanics: a system is no longer able to achieve a range of possible energies as in classical mechanics, rather only a countable subset of energy states are made possible by nature.

The time-dependence of a given state of definite energy, ψ_n, is given by the exponential factor:

$$e^{-iE_n t/\hbar}.$$

Here, E_n is the associated energy of the system in state ψ_n. This exponential factor comes as a result of the separation of variables method used to solve the time-dependent Schrödinger equation and is valid when the Coulomb potential does not vary in time. The stationary states of an atomic system are then written as:

$$\psi_n(\vec{\mathrm{x}}, t) = \psi_{\mathrm{n}}(\vec{x}) \cdot e^{-iE_n t/\hbar}$$

The stationary states are so called because the probability density of such a state has no dependence on time. This is because the conjugate of a complex exponential cancels with itself. Here $\psi_{\mathrm{n}}(\vec{\mathrm{x}})$ is written explicitly to make the distinction that it is a solution of the time-independent Schrödinger equation. E_n is the corresponding energy of $\psi_{\mathrm{n}}(\vec{\mathrm{x}})$. [4]

The simplest and one of the only systems that can be studied analytically is the Hydrogen atom. The treatment of heavier atoms is similar but is much more complex due to the number of variables to be accounted for. From solving the wave equation for

the Hydrogen atom, one finds that in addition to n, there are two quantum numbers that are used to fully characterize the stationary states. The first is orbital angular momentum, denoted by l, which describes the state of the electron as it orbits the nucleus. The second is the magnetic quantum number, denoted m, which corresponds to the magnetic moment of the electron. For a given n, there are n^2 states with unique representations by different values of l and m. From the time-independent Schrödinger equation, the explicit formula for the eigenenergies of the Hydrogen atom is:

$$E_n = -\left[\frac{m}{2\hbar^2}\left(\frac{e^2}{4\pi\varepsilon_0}\right)\right]\frac{1}{n^2}$$

The energy of a stationary state is dependent only on the principal quantum number n. The way the numbers l and m are assigned mean that there are then n^2 states with the same energy. These states are called degenerate states in n, meaning all states identified by a given n will have the same energy. [5]

2.2 Spectra

Introducing external energy into an atomic system, for example shining light on a sample or adding heat, allows for transitions between stationary states to occur. Bringing an electron into an excited state requires that the system absorb energy. Likewise, the reverse process of an electron in an excited state returning to a state of lower energy requires an emission of energy, which is often carried by a photon. During a transition between two states, say ψ_1 and ψ_2 , the atom is in a superposition of these two states:

$$\psi = c_1\psi_1 + c_2\psi_2$$

With c_1 and c_2 varying in time slower than the time varying component of each wavefunction. The probability distribution of this transitory wavefunction is the magnitude of the wavefunction squared:

$$|\psi|^2 = \psi^*\psi = (c_1^*\psi_1^* + c_2^*\psi_2^*)(c_1\psi_1 + c_2\psi_2)$$

$$= \left(c_1^*\psi_1 \cdot e^{iE_1t/\hbar} + c_2^*\psi_2 \cdot e^{iE_2t/\hbar}\right)\left(c_1\psi_1 \cdot e^{-iE_1t/\hbar} + c_2\psi_2 \cdot e^{-iE_2t/\hbar}\right)$$

$$= c_1^2 + c_2^2 + c_1^*c_2\psi_1^*\psi_2 e^{i\omega t} + c_2^*c_1\psi_2^*\psi_1 e^{-i\omega t}$$

with

$$\omega = \frac{E_1 - E_2}{\hbar}$$

This shows that as the electron transits from one stationary state to another, the probability density of its wavefunction is oscillating with a frequency dependent on the difference in energy between those two states. As an atom decays from an excited state to a state of lower energy, a photon corresponding to the energy difference between the two states is emitted. For each emission event, the light emitted is polarized. Because of the random nature of these excitations and decays, the light emitted is overall unpolarized.

Atomic transitions can be observed by sending the emitted light through a spectrometer, which disperses spatially the component wavelengths. A spectrometer records the radiation intensity as a function of wavelength (or photon energy). Spectra are characteristic to their source because the transitions that are recorded are specific to the electronic configuration that allows for them. In addition, the intensities and the

profiles of the spectral lines depend on the source density, temperature, composition, motion, and electromagnetic fields that might be present. For this reason, spectrometers are very useful in astrophysics to determine the conditions of distant stars.

2.3 Fine Structure

With better resolution spectrometers, an interesting feature of the spectra was discovered: what appeared to be a single line was actually multiple closely spaced lines. Prior theory had predicted that there would be multiple transitions with the same energies. It was found that this was not the case and that these transitions actually had slightly different energies. This is known as the fine structure of atomic spectra. Fine structure is a result of intrinsic spin angular momentum of the electron in addition to orbital angular momentum and relativistic effects induced by the fact that the electron moves at speeds comparable to the speed of light. The electron's orbital motion about the nucleus produces an internal magnetic field, which then interacts with the electron's magnetic moment. This manifests itself as closely spaced lines in the spectra of excited atoms. [6]

2.4 Zeeman Effect

The Zeeman Effect is the splitting of energy levels when an atom is placed in an external magnetic field. The degenerate energy levels split as a result of the interaction of the electron's magnetic moment with the external magnetic field. The magnetic field lifts the degeneracies in the magnetic quantum number m. There are three regimes under which the Zeeman effect operates: weak-field, which occurs when the external magnetic field is

small compared to the atom's internal B field; strong-field (also known as the Paschen-Back effect), which occurs when the external field dominates over the internal field; and the intermediate field, in which the fields strengths are comparable. The strong and weak field cases are easiest to treat theoretically as they deal with extreme cases and therefore allow for simplifying assumptions. The intermediate field is the most difficult to discuss because all contributions from both magnetic field and internal fine-structure must be carefully accounted for. What follows is a discussion of the weak-field Zeeman Effect approximation, as it is a generally applicable case and provides a basic understanding of the phenomena at hand.[2] [6]

In the weak-field approximation, spin-orbit (L-S) coupling is much stronger than the external B field. $\vec{L}$ and $\vec{S}$ precess about the total angular momentum, $\vec{J} = \vec{L} + \vec{S}$. The perturbation to the Hamiltonian due to an external B field is given by

$$H' = -(\vec{\mu}_l + \vec{\mu}_s) \cdot \vec{B}$$

Where μ_l is the dipole moment associated with the electron's orbital motion and μ_s is the magnetic moment associated with the electron's spin. The moments are functions of their associated angular momenta, yielding

$$\vec{\mu}_l = -\frac{e}{2m}\vec{L}$$

$$\vec{\mu}_s = -\frac{e}{m}\vec{S}$$

So we can rewrite the perturbation to the Hamiltonian as

[2] Although, the plasmas studied may fall under the strong-field regime as well. Approximating the internal magnetic field of Aluminum by using the Biot-Savart law, $B_{internal} \cong 9$ T.

$$H' = \frac{e}{2m}(\vec{L} + 2\vec{S}) \cdot \vec{B}$$

In quantum mechanics, the perturbation to the energy due to the external B field will be the expected value of the perturbed Hamiltonian

$$E' = \langle \psi_n | H' | \psi_n \rangle = \frac{\mathrm{e}}{2\mathrm{m}} \vec{\mathrm{B}} \langle \vec{\mathrm{L}} + 2\vec{\mathrm{S}} \rangle$$

$\vec{L}$ and $\vec{S}$ are not separately conserved, so we do not know their expectation values explicitly. Instead, we must look at their projections along $\vec{J}$, which is conserved:

$$\vec{S}_{avg} = \frac{(\vec{S} \cdot \vec{J})}{J^2} \vec{J}$$

$$\vec{L}_{avg} = \frac{(\vec{L} \cdot \vec{J})}{J^2} \vec{J}$$

After performing manipulations on the dot products, we are able to write the expectation value of $\vec{L}$ and $\vec{S}$ as an expectation value of S^2, L^2, and J^2, which we know the eigenvalues for. Upon simplification,

$$E' = \frac{e}{2m} \vec{B} \left[1 + \frac{j(j+1) - l(l+1) + s(s+1)}{2j(j+1)} \right] \langle \vec{J} \rangle$$

where $j = l + s$ and l and s are the values of the orbital and spin angular momentum of the state involved. Arbitrarily choosing B to lie along the z-axis, we then are able to replace the expectation value of $\vec{J}$ with its eigenvalue, $m_j \hbar$:

$$E' = \mu_B g_j B m_j$$

where

$$g_j = \left[1 + \frac{j(j+1) - l(l+1) + s(s+1)}{2j(j+1)}\right]$$

is the Lande g-factor and

$$\mu_B = \frac{e\hbar}{2m}$$

is the Bohr magneton. [7]

2.5 Zeeman Broadening

Theoretically, a measurement of the splitting of the spectral lines will yield the strength of the magnetic field present in the source. However, in the plasma systems we are interested in studying, there are other mechanisms at play also affecting the spectral line profiles. In these cases, the spectral pattern created by the Zeeman Effect may become overwhelmed by other line-broadening mechanisms. Examples of competing mechanisms include the Stark Effect and Doppler broadening. The Stark Effect is analogous to the Zeeman Effect, except with an electric field as the perturbation that broadens the spectral line profiles. Doppler broadening occurs as a result of the motion of the emitting ions with respect to the observer. Along the line of sight of the spectrometer, some of the ions are moving towards the instrument while others are moving away. [8,9] Thus, the ions moving at velocity v will emit frequency ω that is shifted from the rest frequency ω_0 as described by the Doppler equation:

$$\omega = \omega_0(1 \pm \frac{v}{c})$$

One interesting property of atomic spectra that we intend to take advantage of is that different fine structure components are affected equally by other broadening mechanisms but differently by the Zeeman Effect. This allows us to obtain magnetic field measurements in plasmas whose spectra are simultaneously being broadened by these other mechanisms. [10]

Different fine structure components differ in total angular momentum, *j*. The Lande g-factor which determines the shift in energy due to an external B field,

$$g_j = \left[1 + \frac{j(j+1) - l(l+1) + s(s+1)}{2j(j+1)}\right]$$

is a function of *j*. Due to this fact, the difference between the line broadening of different multiplet components provides a direct measurement of the field strength.

III. Experimental Set-Up

3.1 Zebra

The Nevada Terawatt Facility houses the two terawatt pulsed power generator Zebra[3], Figure 1, used to create the magnetic fields to be studied in this experiment. Zebra is able to generate a one mega-ampere (1 million amperes) current pulse that reaches maximum current in 100 nanoseconds. It does so by starting with a microsecond current pulse and sending it through three stages of power amplification. Because power is equal to energy divided by time, the key to increasing power is shortening the time in which an amount of energy is transferred. The first of these stages is charging up thirty-

[3] Zebra was generously donated to the University of Nevada, Reno by Los Alamos National Laboratories with the intention of allowing students research opportunities on this advanced machine. [13]

two 1.3 μF capacitors in parallel and discharging them in series. This configuration of capacitors is known as the Marx capacitor bank. The total energy stored is 200 kilojoules. The second stage is a coaxial 28 nF, 3.5 MV capacitor (intermediate storage) that is submerged in water which it uses for a dielectric. Once this capacitor is 80% charged, a self-triggered electrical switch (rimfire switch) allows it to discharge into the final stage of power amplification (vertical transmission line). The current pulse is further compressed as it is sent through water spark-gaps and finally applies two million volts onto the load, which is situated inside the vacuum chamber.

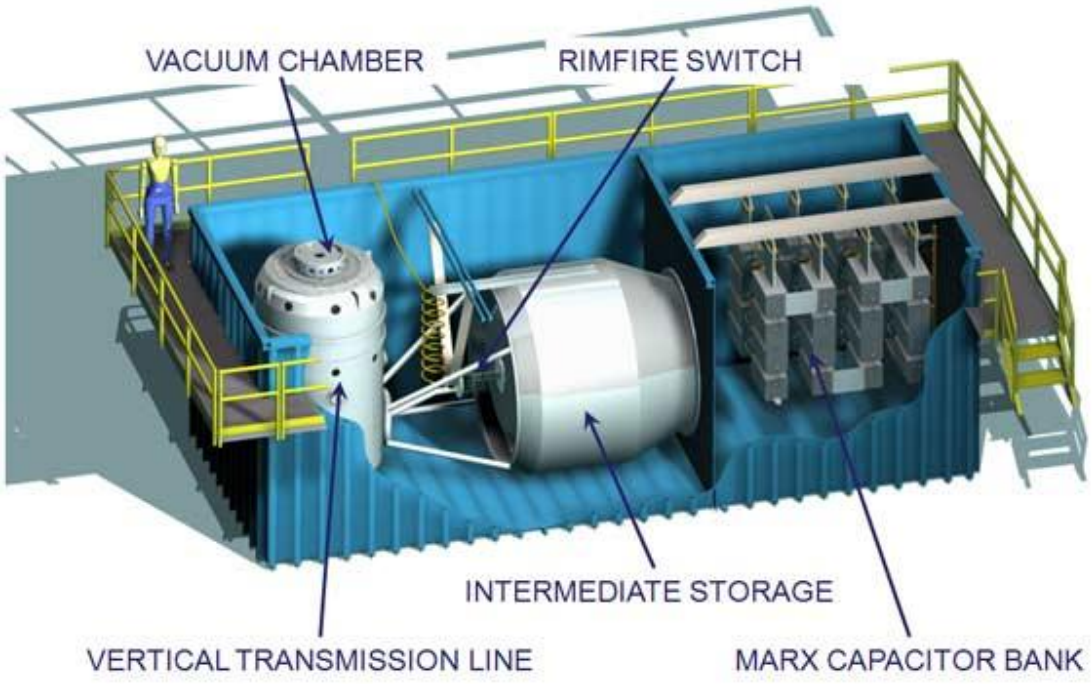

Figure 1. The Zebra Machine at the Nevada Terawatt Facility.

3.2 Methods

Plasma was created by ablating various aluminum wire array loads heated by the Zebra current pulse. The transition selected for examination are the

$2p^6 4s\ ^2S_{1/2} - 2p^6 4p\ ^2P_{1/2,3/2}$ doublet components of Al III (569.7 and 572.3 nm). The Zeeman broadenings of these transitions can be used for plasma densities up to $n_e = 10^{18}$ cm^{-3}, plasma temperature up to $T_e = 10$ eV, and magnetic field strengths up to 40 Tesla.

The wire arrays used were cylindrical arrays, conical arrays, and x-pinches made of 15 micrometer diameter Aluminum wires. The cylindrical and conical arrays were made of eight wires and the x-pinch of four. The dimensions of the arrays are approximately one centimeter in diameter and two centimeters high.

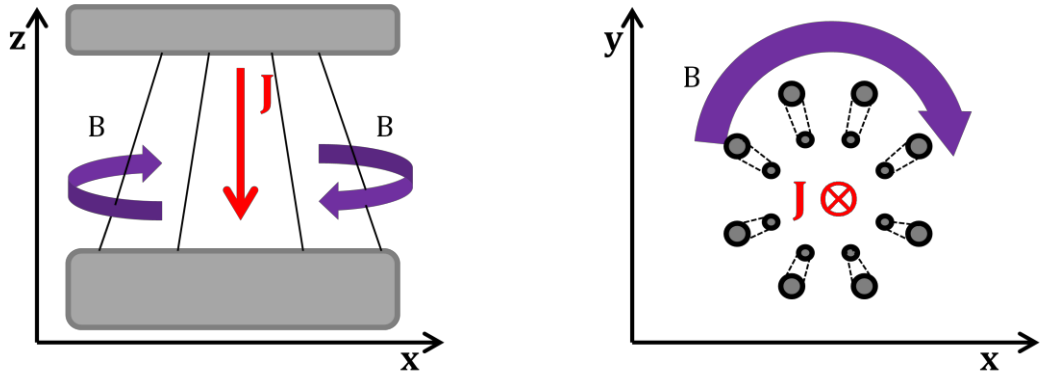

Figure 2: Typical load setup.
Drawing of load setup for inverted conical wire array. The x-z axis represents a side-view of the array and the x-y axis depicts a top-view of the load showing the 8 symmetric wires. The direction of the Zebra current J and azimuthal magnetic field B are indicated.

3.3 Diagnostics

Our primary diagnostic is a high resolution one-meter Acton Research spectrometer to analyze the doublet components. Our spectra were recorded on a gated optical camera with a gate of ~100 nanoseconds. The spectra had space resolution along the array diameter, and the portion of the load that was analyzed can be seen on images taken by a second diagnostic, the gated optical imager (GOI). The latter used a second ICCD to record the self-emission from the wire array load immediately before it entered

the spectrometer by use of a beam-splitter. In addition, broadband time- and space-integrated spectra were obtained to determine whether other doublet transitions looked promising for further investigation with the high resolution instrument. Secondary diagnostics included Faraday rotation and interferometry. The pulsed probing beam for these diagnostics had a 532 nanometer wavelength, 90 millijoule energy, and 0.2 nanoseconds duration. The line-of-sight for the laser images was perpendicular to the line-of-sight of the spectrographs.

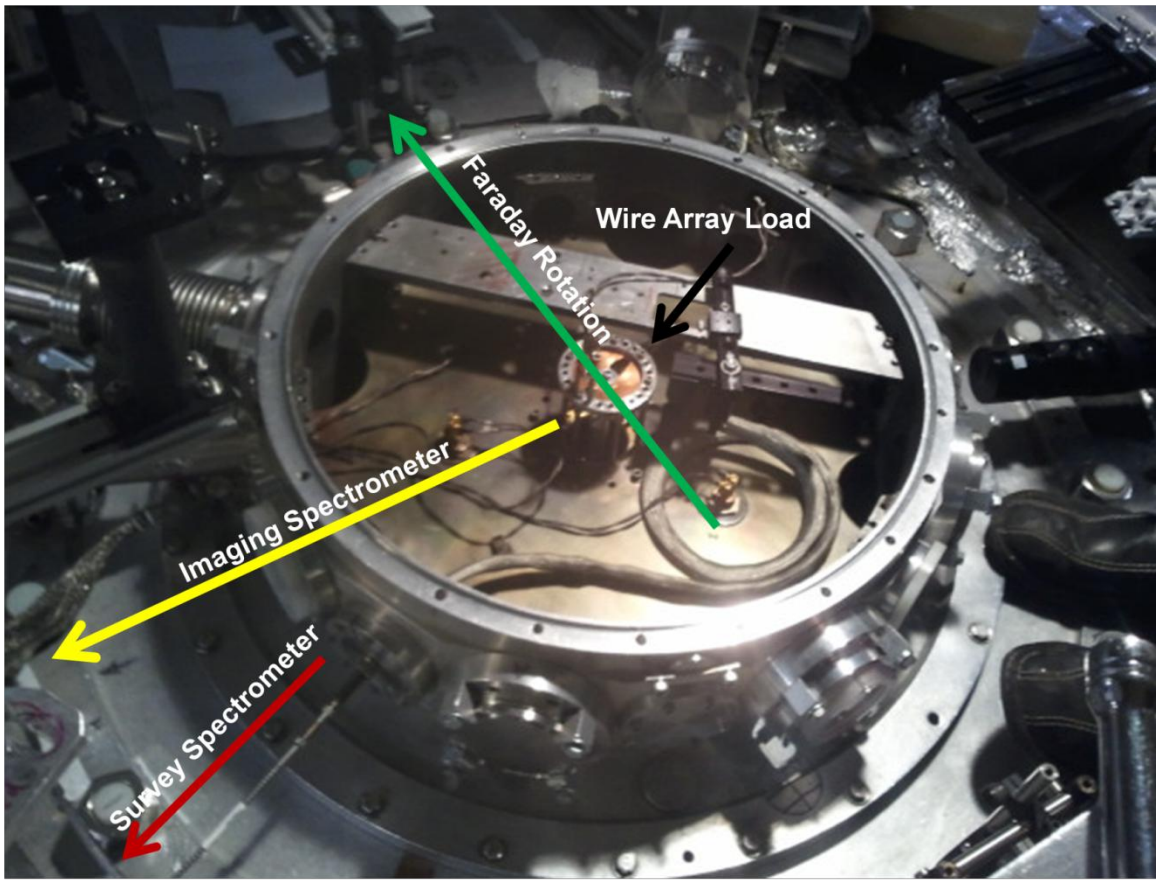

Figure 3: Line-of-sight views of diagnostics employed.

IV. Results

The spectrograms were analyzed by first removing background from the image by use of the image manipulation software, ImageJ[4]. ImageJ's built in background removal tool makes use of the rolling-ball algorithm, which is optimized for removing non-uniform background. [11] Next, an average line profile was taken along the imaging direction so as to maximize pixel counts.

4.1 Zebra Shots 3012 and 3024

Shown are the GOI images, raw high-resolution spectra and processed line profiles of two Zebra shots. The drawn-in axes show along which axis spatial resolution is preserved and along which axis wavelength resolution is obtained. The intensities plotted of the spatially averaged wavelength are given by the pixel values of the raw image. Unfortunately, the axis of the image on the slit of the spectrometer was not normal to the slit, but rotated by approximately three degrees. The spectrometer entrance slit was opened to 50 micrometers. The region of the self-emission image that entered the spectrometer is shown approximately.

[4] ImageJ is an public domain image processing software developed at National Institutes of Health (NIH).

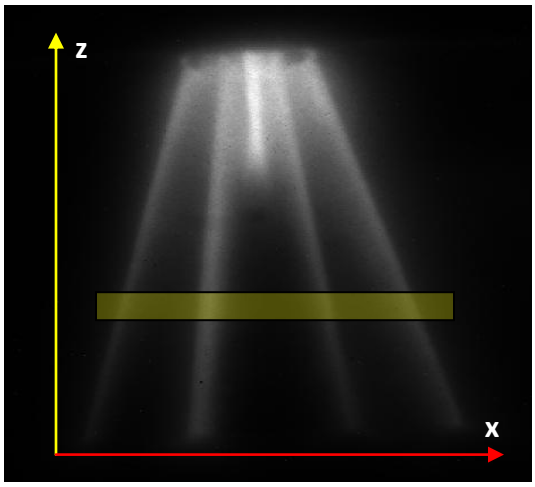

Figure 4: Shot 3013 Gate image.
Image of self-emission from an inverted conical wire array made of 8-15 μm Al wires. The highlighted yellow region shows approximately the position of the spectrometer slit. The image was acquired over 100ns.

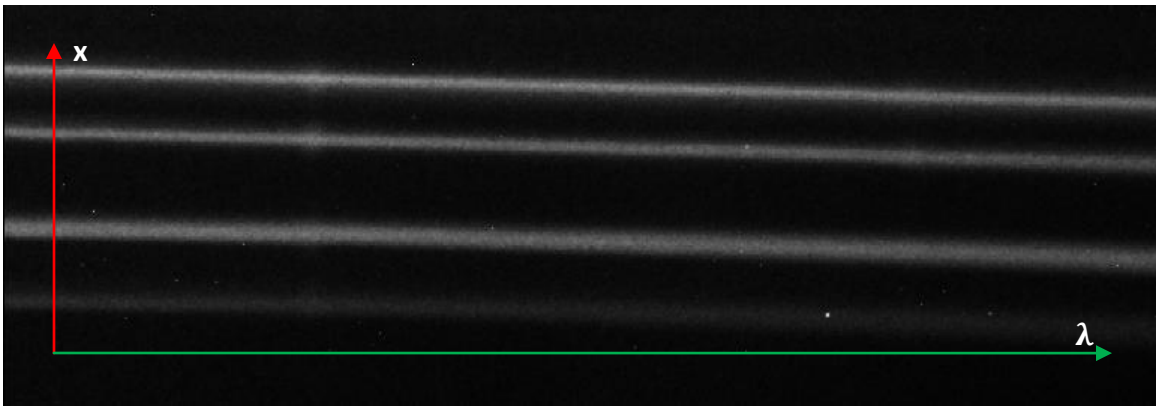

Figure 5: Shot 3013 time-integrated spectrum.
For this spectrogram, the spectrometer was centered at 571nm with an entrance slit size of 50 micrometers. The image was taken with a 100ns gate. The labeled x-axis corresponds to the same red x-axis along the diameter of the load in Figure 4.

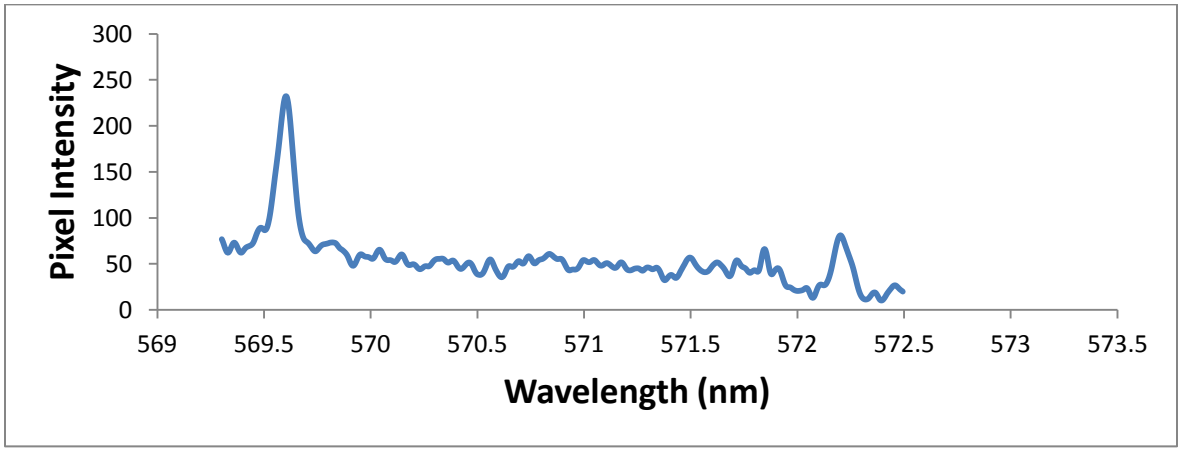

Figure 6: Shot 3013 spectrum.
A plot profile was taken of the spectrogram (Figure 5) by averaging along the x-axis. Pixel intensity units are arbitrary.

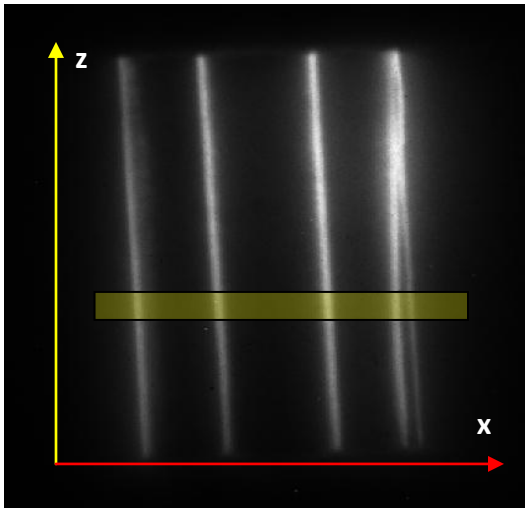

Figure 7: Shot 3024 Gate image.
Image of self-emission from cylindrical wire array made of 8-15 µm Al wires. The highlighted yellow region shows the part of the image that was analyzed by the spectrometer (Figure 8). This image, too, was acquired over 100ns.

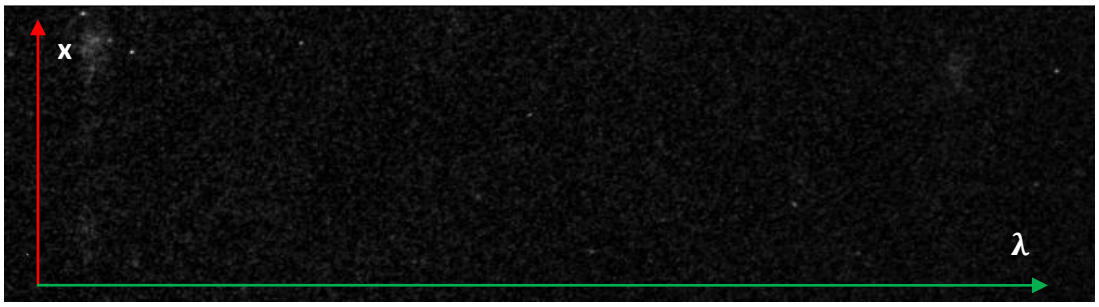

Figure 8: Shot 3024 time-integrated spectrum.
For this spectrogram, the spectrometer was centered at 571nm with an entrance slit size of 250 micrometers. The image was taken with a 100ns gate. The labeled x-axis corresponds to the same axis along the diameter of the load in Figure 7. More evident in this image than in Figure 5 are the two emission lines of the doublet transition.

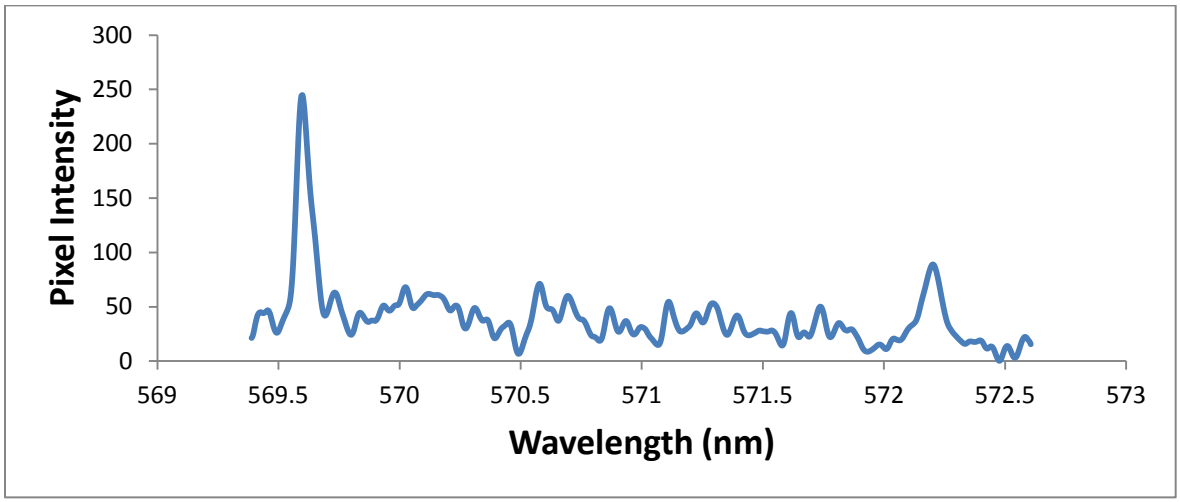

Figure 9: Shot 3024 spectrum.
A plot profile was taken of the spectrogram (Figure 8) by averaging along the x-axis. Pixel intensity units are arbitrary.

One can see that even the processed spectra of Figures 6 and 9 are very noisy. This makes analysis difficult, as it becomes unclear where data from an emission event occurs and where it is simply background. To compare the widths of the two peaks, it is necessary to compare the full width at half maximum (FWHM) values of each peak. These shots were chosen because they appear to be promising candidates for peak width difference detection.

4.2 Future Work

Preliminary analysis of the spectra indicates width differences between the two doublet components. This is not definitive, however, and further processing must be done to verify. The magnetic fields present during this experiment may have been too weak for the spectral lines to sufficiently exhibit Zeeman broadening. Changing the load configuration is one improvement for future experiments by changing the field strengths being produced.

Figure 10 shows a theoretical calculation of the effect various B fields will have on the specific doublet we were looking at, courtesy of S. Hansen. [12] This shows the difference in peak widths of the two doublet components we should expect to see. In comparing our raw data to this model, it should be noted that the responses in peak widths and intensities are similar for field strengths of approximately ≤ 5 Tesla.

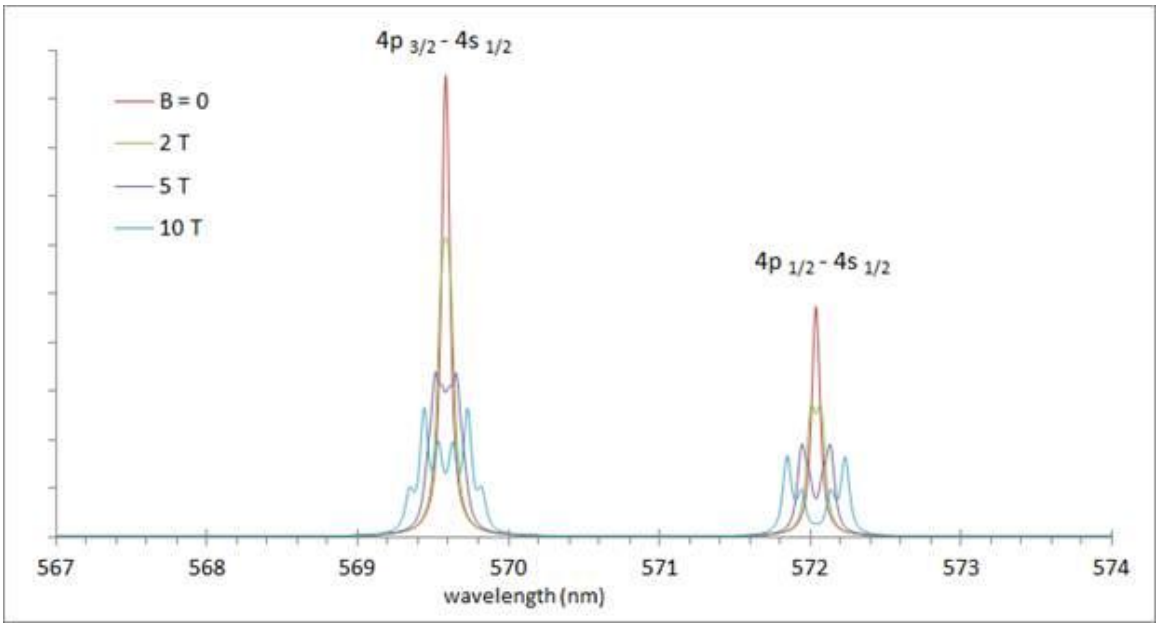

Figure 10: Model of effect of isotropic B field on Al doublet

V. Conclusions

The goal of this work is to develop a diagnostic that will become standard in plasma experiments at the NTF and in magnetized high energy density plasma experiments in general. This diagnostic will be extremely useful as it provides information about magnetic fields that is necessary but not accessible. One of the most challenging tasks in experimental physics is the refinement of a certain technique. With so many variables and binding constraints to adhere to, a certain degree of error is inevitable. Minimizing this error will be the primary focus of this project, so as to produce results that are consistently precise and accurate. Once we are able to apply this diagnostic to other experiments exploring plasma-magnetic field systems, the additional pieces of data obtained as a result may influence the direction of ongoing projects.

VI. Acknowledgements

This work was supported by the DOE/OFES grant DE-SC0008829 and DOE/NNSA contract DE-FC52-06NA27616.

I would additionally like to thank R. Presura, T. Valentine, M. Wallace, N. Quiros, A. Arias, and the NTF Management and Technical Team for their help, time, support and patience in my endeavors.

VII. References

1. Miyamoto, K., *Plasma Physics and Controlled Nuclear Fusion*. Germany: Springer Berlin Heidelberg New York. 2005.
2. Miller, M.C. Introduction to Neutron Stars. *Department of Astronomy, University of Maryland* at <http://www.astro.umd.edu/~miller/nstar.html>.
3. Tessarin, S. (2011). Beyond Zeeman spectroscopy: Magnetic-field diagnostics with stark-dominated line shapes. *Physics of Plasmas*, *18*, doi: 10.1063/1.3625555
4. Fowles, Grant R. *Introduction to Modern Optics*. 2nd ed. New York: Dover Publications, Inc., 1968. 226-261. Print.
5. Richtmyer, F.K., and E.H. Kennard. *Introduction of Modern Physics*. 4th ed. New York: McGraw-Hill Book Company, Inc., 1947. 329-345. Print.
6. Griffiths, D. J. *Introduction to quantum mechanics*. 2nd. Upper Saddle River, New Jersey: Pearson Prentice Hall, 2005. 266-276. Print.
7. Griffiths, D. J. *Introduction to quantum mechanics*. 2nd. Upper Saddle River, New Jersey: Pearson Prentice Hall, 2005. 277-283. Print.
8. Fantz, U. (2006). Basics of plasma spectroscopy. *Plasma Sources Science and Technology*, 15. doi: 10.1088/0963-0252/15/4/S01
9. McLean, E., Stamper, J., Manka, C.K., Griem, H.R., Droepmer, D.W., & Ripin, B.H. (1984). Observation of magnetic fields in laser-produced plasma using Zeeman effect. *Physics of Fluids*, 27. doi: 10.1063/1.864747
10. Stambulchik, E., Tsigutkin, K., & Maron, Y. (2007). Spectroscopic Method for Measuring Plasma Magnetic Fields Having Arbitrary Distributions of Direction and Amplitude. *Physical Review Letters*, 98(22), 225001. doi: 10.1103/PhysRevLett.98.22501
11. Castillejo, Marta. *Lasers in the Conservation of Artworks*. London: CRC Press, 2008. 104-106. eBook.
12. Hansen, S. "Zeeman Splitting in Al lines." Private communication to Showera Haque. 09 April 2013. E-mail.
13. J.S. Shlachter, (1990). Solid D_2 Fiber Experiments on HDZP-II. *Plasma Physics and Controlled Fusion,* 32, 1072-1081.